

ZHENG Ke-yu, WEI Nian, YANG Feng-xia, QI Ya-jun,
ZHANG Duan-ming

$\text{KTa}_{0.4}\text{Nb}_{0.6}\text{O}_3$ nanoparticles synthesized through solvothermal method

© Higher Education Press and Springer-Verlag 2007

Abstract Potassium tantalate niobate ($\text{KTa}_{0.4}\text{Nb}_{0.6}\text{O}_3$, KTN) nanoparticles of perovskite structure were successfully synthesized by a solvothermal method. The KTN nanoparticles synthesized at 250 °C for 8 h with 1 to 4 M KOH concentration using isopropyl alcohol [$(\text{CH}_3)_2\text{CHOH}$] as the solvent was composed of a single phase of cubic perovskite structure. Furthermore, the KTN powders synthesized at the same conditions besides of using $(\text{CH}_3)_2\text{CHOH}/\text{H}_2\text{O}$ as a solvent compose of a single phase of tetragonal perovskite structure. The nanoparticles exhibit a mixture of cubic and prism-like shapes with lengths of 100 nm to 500 nm and average cross sections of $200 \times 200 \text{ nm}^2$. The solvent dependence of the powder formation is discussed. X-ray diffraction and electron diffraction results show that the powders have the needed tetragonal perovskite structure. The band gap of KTN nanoparticles is determined to be 3.26 eV from the optical absorption spectra.

Keywords $\text{KTa}_x\text{Nb}_{1-x}\text{O}_3$, solvothermal, nanoparticles

PACS numbers 73.63.Bd

1 Introduction

Perovskite-type solid solution potassium tantalate niobate ($\text{KTa}_{1-x}\text{Nb}_x\text{O}_3$ generally known as KTN) have received a great deal of attention owing to their piezoelectric, pyroelec-

tric, and electro-optic properties. KTN crystals are used in many important fields such as volume phase holographic storage, real-time optical information processing, IR detectors, electro-optic devices, and so on [1–4]. Over the past few decades, KTN thin films of perovskite structure have been successfully prepared using different procedures including chemical solution deposition (CSD), chemical vapor deposition (CVD), Sol-Gel, and pulsed laser deposition (PLD) methods [5–9]. The fabrication cost of KTN thin films is too high because of the costly metal-organic compounds used. On the other hand, producing KTN ceramics with desirable properties is very difficult, and the stoichiometric ratio of KTN easily deviates, because the potassium component is volatilizable at high reactive temperature.

Hydrothermal techniques have also been proposed for obtaining many kinds of nanocrystalline materials [10, 11]. Compared to the techniques mentioned above, hydrothermal methods have several advantages: simplifying process from cheap raw materials and comparatively low reactive temperature. Recently, we synthesized nanocrystalline KTN using a simpler single-process starting from Ta_2O_5 , Nb_2O_5 and KOH by the solvothermal method. The solvothermal method is one way of Hydrothermal techniques, and it was hardly reported that the KTN nanopowders were obtained with this means. The formation of pyrochlore phase should be avoided in the preparation. This paper presents the preparation of a series of KTN powders, and their characterization by X-ray diffraction (XRD) and transmission electron microscopy (TEM).

ZHENG Ke-yu, WEI Nian, YANG Feng-xia, ZHANG Duan-ming (✉)
Physics Department, Huazhong University of Science and Technology,
Wuhan 430074, China
E-mail: zhangd@public.wh.hb.cn

ZHENG Ke-yu, QI Ya-jun
Faculty of Materials Science & Engineering and Hubei Key Laboratory
of Ferroelectric and Piezoelectric Materials and Devices,
Hubei University, Wuhan 430062, China

Received January 15, 2007

2 Experimental

Nb_2O_5 and Ta_2O_5 with high purity were chosen as starting materials for the synthesis of KTN powders. KOH was used as a mineralizer and a starting material for the solvothermal synthesis. $(\text{CH}_3)_2\text{CHOH}$ and H_2O were chosen as the solvent. Stoichiometric amounts of Nb_2O_5 and Ta_2O_5 solution were put into a 50-mL Teflon-lined autoclave. Then, KOH was

dissolved in the solvent and added into the Teflon-lined autoclave slowly with stirring. The resulting solutions were adjusted to different pH values (KOH concentration 0.5–4 M) by mixing with KOH and filled with $(\text{CH}_3)_2\text{CHOH}/\text{H}_2\text{O}$ to less than 80 % of its capacity. The final mixtures were stirred for 30 min. Finally, the autoclave was maintained at 250 °C for 8 h, and then cooled to room temperature naturally. The resulting precipitate was filtered using a vacuum filter, washed with deionized water several times, and dried in an oven at 80 °C for 12 h.

X-ray diffraction (XRD) patterns of powders were recorded on a PHILIPS X'pert Pro X-ray diffractometer with $\text{Cu K}\alpha$ radiation ($\lambda = 1.546 \text{ \AA}$). Transmission electron microscopy (TEM) images and electron diffraction (ED) patterns were carried out on a Tecnai G20 electron microscope operated at 200 kV. The UV–Visible absorption spectrum was obtained on a UV–Visible spectrophotometer (UV-2550, SHIMADZU, Japan). BaSO_4 was used as a reflectance standard in the UV–Vis diffuse reflectance experiment.

3 Results and discussion

X-ray diffraction patterns of KTN powders synthesized with various KOH concentrations at 250 °C for 8 h using $(\text{CH}_3)_2\text{CHOH}$ as the solvent are shown in Fig. 1. When the KOH concentration is higher than 0.5 M, the five main peak at 2θ values of 22.3°, 31.6°, 45.2°, 51.1°, and 56.4° can be indexed as (100), (110), (200), (210), and (211) of the cubic phase structure of KTN, with a good agreement with the data of the JCPDS file (JCPDS card No. 710945). The thimbleful pyrochlore phase and the remains of Ta_2O_5 (JCPDS card No. 892843) were detected when the KOH concentration was 0.5 M or even lower (not shown here). No other diffraction peaks were present in Fig. 1 (1 M, 2 M KOH), indicating that the product is a single phase of cubic perovskite structure with KOH concentration higher than 1 M. Lu *et al.* demonstrated that the pyrochlore phase exist throughout the anneal treatment of KTN thin films [8]. The pyrochlore phase in KTN particles synthesized using $(\text{CH}_3)_2\text{CHOH}$ as solvent was easily eliminated.

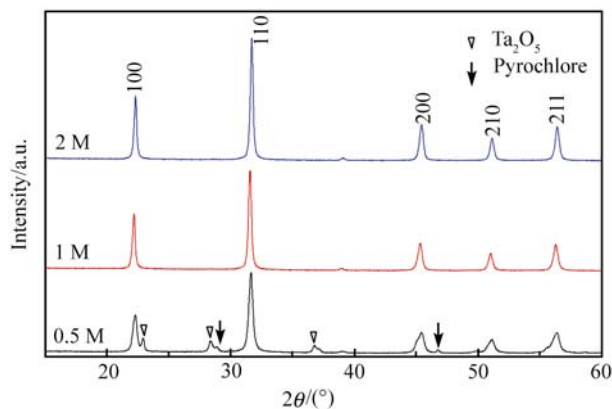


Fig. 1 XRD patterns of KTN nanoparticles synthesized at 250 °C with a solvent of pure isopropyl alcohol using various KOH concentrations.

Figure 2 shows XRD patterns of KTN powders obtained at 250 °C for 8 h with different ratios of $(\text{CH}_3)_2\text{CHOH}$ to H_2O and 4 M KOH concentration. It can be seen that the intensities of the diffraction peaks decrease with the increase of H_2O content. More importantly, when the ratio of $(\text{CH}_3)_2\text{CHOH}$ to H_2O reached 60/40 the pyrochlore phase and other phases such as Ta_2O_5 , $\text{K}_2\text{Ta}_2\text{O}_6$ (JCPDS card No. 351464) appeared. However, the XRD of the obtained particles formed with the ratio of 90/10 confirmed the tetragonal phase perovskite structure. As shown in the inset of Fig. 2, the peak of (002) and (200) can be distinguished clearly. The observed peaks were similar to the crystallographic structure of tetragonal phase KN. As shown in Fig. 1, the product synthesized using pure isopropanol as a solvent were all cubic perovskite structures with a KOH concentration higher than 1 M. In our previous works, the formation of tetragonal phase KTN occurred effectively in the high alkaline medium (7 M KOH) at a long reaction time of 24 h [12, 13], using pure water as the solvent. It seems that the solvents play an important role in the formation of the KTN phase. The critical temperature of $(\text{CH}_3)_2\text{CHOH}$ is lower than that of water; the $(\text{CH}_3)_2\text{CHOH}$ solvent may reach its critical point in solvent hydrothermal condition and accelerate the solvent of the starting materials and then expedite reactive velocity.

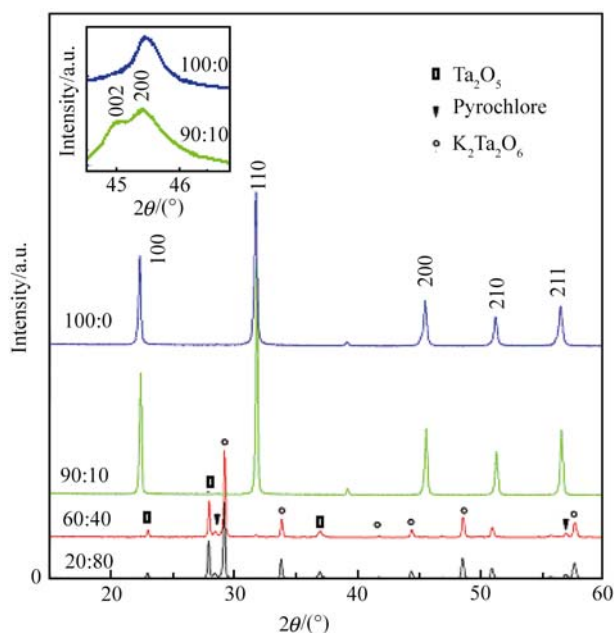


Fig. 2 XRD patterns of KTN nanoparticles synthesized at 250 °C 4 M KOH with various $(\text{CH}_3)_2\text{CHOH}/\text{H}_2\text{O}$ ratios. The enlarged {200} diffraction peaks are in the inset.

The scanning electron microscopy (SEM) image of KTN nanoparticles synthesized at 250 °C 2 M KOH using pure isopropanol is shown in Fig. 3, from which a cubic morphology or a prism-like shape can be found. The length sizes of the particles are in the range of 100 to 500 nm and the average cross section is about $200 \times 200 \text{ nm}^2$.

Figure 4 shows the TEM image of KTN nanoparticles

synthesized at 250°C for 8 h using 4 M KOH with (CH₃)₂CHOH/H₂O ratio 90:10. As shown in Fig. 4 (a), the KTN particles exhibit a mixture of cubic and prism-like shapes with a size of 100–500 nm, which is in accordance with the observation by SEM. According to XRD results at the ratio of 90/10, the as-prepared KTN should possess a tetragonal phase perovskite, confirmed by the SAED patterns. As shown in Fig. 4(b) and (c), the SAED patterns along [010] and [1 $\bar{1}$ 0] zones indicate the single crystal nature of KTN nanoparticles with a tetragonal phase.

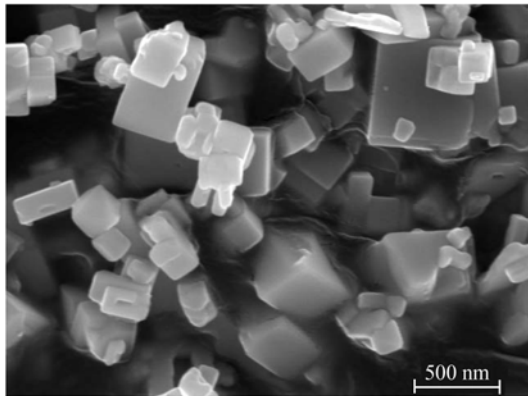


Fig. 3 SEM image of KTN nanoparticles synthesized at 2 M KOH concentration using pure isopropyl alcohol as the solvent.

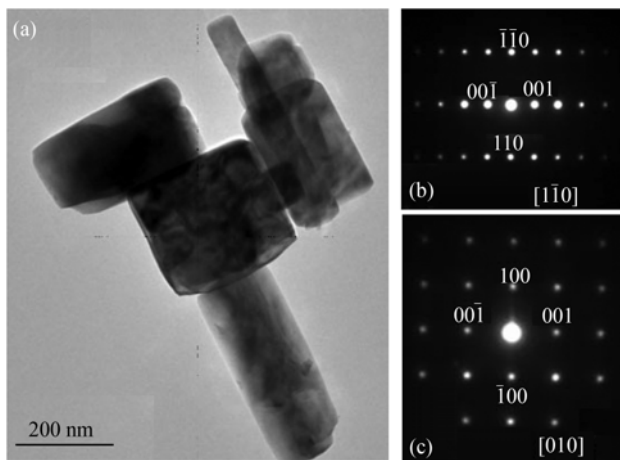


Fig. 4 TEM image of KTN nanoparticles using 4 M KOH with (CH₃)₂CHOH/H₂O ratio 90:10 and the corresponding SAED patterns.

Figure 5(a) shows the light absorption characteristics of the KTN particles in the UV and visible regions. Well-defined bands with peaks can be seen at 5.5 to 4.2 eV. The absorption coefficient A as a function of photon energy can be expressed by the Tauc relation [14]:

$$Ahv = C(hv - E_g)^n \quad (1)$$

where C is constant, E_g is the allowed energy gap, $h\nu$ is the photon energy and n is an index determined by the nature of the electron transition during the absorption process. It is well known that there are two types of fundamental optical

transitions, namely direct ($n = 1/2$) and indirect ($n = 2$). For KTN, it is a direct band-gap semiconductor, so here $n = 1/2$. The plot of $(Ahv)^2$ versus $h\nu$ is presented in Fig. 5(b). The optical band-gap E_g is obtained by extrapolating the straight-line portion of the plot at $Ah\nu = 0$. The E_g value of KTN is determined to be 3.26 eV. The result shows a blue shift from the relevant absorption band 2.0 eV of Ti doped KNbO₃ crystals [15] and it may be due to the quantum-size effect.

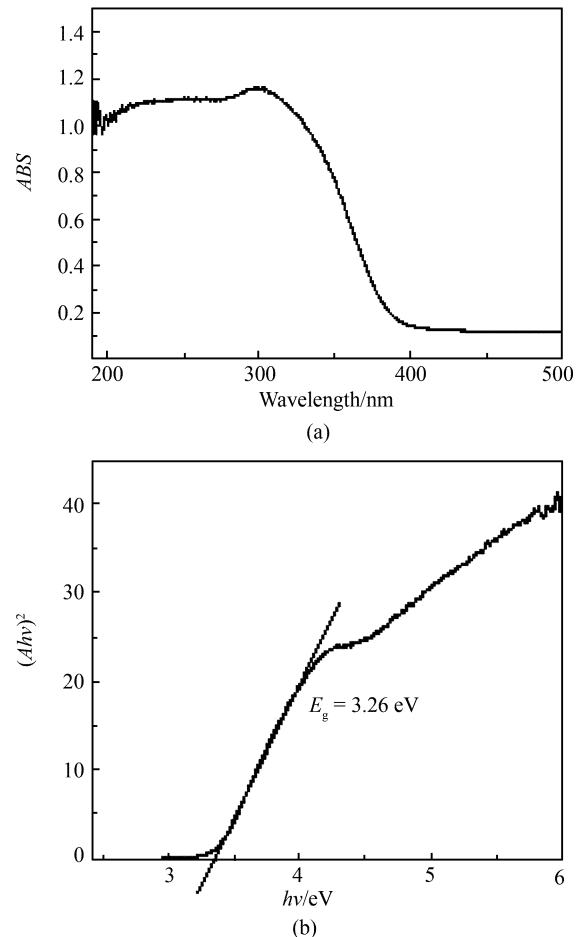


Fig. 5 UV-Vis absorption spectrum (a) and plot of $(Ahv)^2$ versus $h\nu$ of KTN nanoparticles (b).

4 Conclusion

KTa_xNb_{1-x}O₃ ($x = 0.4$) nanoparticles of perovskite structure were successfully synthesized by a solvothermal method. It was found that solvents play an important role in the formation of KTN phase. The KTN nanoparticles of single phase cubic perovskite structure were obtained with 1–4 M KOH concentration using isopropyl alcohol as a solvent, while tetragonal phase was formed when the ratio of (CH₃)₂CHOH to H₂O reached 90/10. The nanoparticles exhibit a mixture of cubic and prism-like shapes with lengths from 100 to 500

nm and average cross sections of $200 \times 200 \text{ nm}^2$. The band gap of KTN nanoparticles is determined to be 3.26 eV from the optical absorption spectra.

Acknowledgements This work was supported by the Open Program of Hubei Key Laboratory of Ferro- and Piezoelectric Materials and Devices.

References

1. Bao D., Kuang A., and Gu H., *Phys. Status Solidi (a)*, 1997, 163: 67
2. Hirano S., Yogo T., Kikuta K., Morishita T., and Ito Y., *J. Am. Ceram. Soc.*, 1992, 75: 1701
3. Lu C. J. and Kuang A. X., *J. Mater. Sci.*, 1997, 32: 4421
4. Suzuki K., Sakamoto W., Yogo T., and Hirano S., *J. Am. Ceram. Soc.*, 1999, 82: 1463
5. Zhang D. M., Li Z. H., Wang X. D., et al., *Am. Ceram. Soc. Bull.*, 2001, 80(2): 57
6. Buršik J., Železný V., and Vaněk P., *Journal of the European Ceramic Society*, 2005, 25: 2151
7. Tadayuki Imai, Shogo Yagi, et al., *Journal of Crystal Growth*, 1995, 147: 350
8. Lu C. J., Kuang A. X., Huang G. Y., and Wang S. M., *J. Mater. Sci.*, 1996, 31(12): 3081
9. Kuang A. X., Lu C. J., Huang G. Y., and Wang S. M., *J. Crystal Growth*, 1995, 149: 80
10. Ganesh Suyal, Enrico Colla, Roman Gysel, Marco Cantoni, and Nava Setter, *Nano Letters*, 2004, 4(7): 1339
11. Salminen J. and Antson O., *Ind. Eng. Chem. Res.*, 2002, 41: 3312
12. Wang Y. X., Zhong W. L., Wang C. L., et al., *Optics Communications*, 2002, 201: 79
13. Nitin P. Padture and Wei X. Z., *J. Am. Ceram. Soc.*, 2003, 86(12): 2215
14. Tauc J. C., *Optical Properties of Solids*, North-Holland, Amsterdam, 1972: 372
15. Kotomin E. A., et al., *Computational Materials Science*, 2000, 17: 290